ELSEVIER

Journal of Structural Geology 27 (2005) 89–100

JOURNAL OF STRUCTURAL GEOLOGY

www.elsevier.com/locate/jsg

Experimental microstylolites in quartz and modeled application to natural stylolitic structures

J.P. Gratier[a,*], L. Muquet[a], R. Hassani[b], F. Renard[a,c]

[a]*LGIT, CNRS-Observatoire, Geosciences, Université Joseph Fourier, BP 53, 38041 Grenoble, France*
[b]*LGCA, CNRS-Observatoire, Université de Savoie, 73376 Le Bourget du Lac, France*
[c]*Physics of Geological Processes, University of Oslo, Norway*

Received 28 May 2003; received in revised form 31 May 2004; accepted 31 May 2004

Abstract

Experimental microstylolites have been observed at stressed contacts between quartz grains loaded for several weeks in the presence of an aqueous silica solution, at 350 °C and 50 MPa of differential stress. Stereoscopic analysis of pairs of SEM images yielded a digital elevation model of the surface of the microstylolites. Fourier analyses of these microstylolites reveal a self-affine roughness (with a roughness exponent H of 1.2). Coupled with observations of close interactions between dissolution pits and stylolitic peaks, these data illustrate a possible mechanism for stylolite formation. The complex geometry of stylolite surfaces is imposed by the interplay between the development of dissolution peaks in preferential locations (fast dissolution pits) and the mechanical properties of the solid–fluid–solid interfaces.

Simple mechanical modeling expresses the crucial competition that could rule the development of microstylolites: (i) a stress-related process, modeled in terms of the stiffness of springs that activate the heterogeneous dissolution rates of the solid interface, promotes the deflection. In parallel, (ii) the strength of the solid interface, modeled in terms of the stiffness of a membrane, is equivalent to a surface tension that limits the deflection and opposes its development. The modeling produces stylolitic surfaces with characteristic geometries varying from conical to columnar when both the effect of dissolution-rate heterogeneity and the strength properties of the rock are taken into account. A self-affine roughness exponent ($H \approx 1.2$) measured on modeled surfaces is comparable with natural stylolites at small length scale and experimental microstylolites.

Keywords: Stylolites; Pressure solution; Quartz; Aqueous silica solution

1. Introduction

Stylolites are well known as natural markers of pressure solution. Following the interpretation of Stockdale (1922), relating stylolite development to stress-driven dissolution, there has been general agreement about such an explanation (Dunnington, 1954; Heald, 1955; Park and Schot, 1968; Arthaud and Mattauer, 1969; Carrio-Schaffhauser et al., 1990; Dewers and Ortoleva, 1990a,b). Nonetheless, some authors also suggested that cataclastic deformation could contribute to the specific stylolitic shape (Deelman, 1976; Milliken, 1994). Based on the observation of roughly regular spacing, the development of stylolitic layering surfaces has been related to self-organized processes (Merino et al., 1983; Dewers and Ortoleva, 1990a), with such processes arising from stress-induced instability in chemically compacting rocks and leading to the formation of spatial heterogeneity in rock. However, this type of model has been questioned by other authors who consider either that the spacing of stylolites is indistinguishable from random arrangement (Railsback, 1998) or that initial conditions (e.g. fracture patterns) could impose a rough regular spacing (Railsback and Andrews, 1995). The intriguing stylolitic tooth-like shape itself has been interpreted as a self-organized process linked to the interplay between stress state variations and progressive changes of rock porosity (Gratier, 1987). Due to the well-recognized role of stylolites in compaction and creep processes

* Corresponding author. Fax: +33-476-82-81-01
E-mail address: gratier@lgit.obs.ujf-grenoble.fr (J.P. Gratier).

0191-8141/$ - see front matter © 2004 Published by Elsevier Ltd.
doi:10.1016/j.jsg.2004.05.007

(Bathurst, 1971), it is important to decipher the effect of the various parameters in their development.

Many previous studies have been performed on natural stylolitic structures. In such cases, information on crucial parameters, mainly those concerning initial state, mechanical behavior, stress-state and dissolution-rate are missing. This is why trying to obtain experimental stylolites by controlling primary parameters in the laboratory could help in understanding their development. However, the very slow kinetics of pressure solution processes (Rutter, 1976) makes them very difficult to reproduce. This paper presents experimental microstylolite surfaces that formed along stressed grains contacts. Such experimental microstylolites are developed to the extent that they can be studied as closely as natural stylolite surfaces. From the geometric analysis of such experimental microstylolite surfaces a conceptual model for stylolite development has been proposed and tested.

2. Experiments

Transparent euhedral quartz crystals collected from tension gashes in the Oisans massif (French Alps), were ground and the 100–125 micron fraction was selected. Layers of those fine quartz sand grains were sandwiched between cylindrical samples of quartzite, flooded with a silica solution, then loaded for several weeks under a vertical uniaxial stress (σ_1) of 200 MPa (Fig. 1a). Experiments were run in pressure vessels at a temperature of 350 °C and a fluid pressure (P) of 150 MPa. Thin sections of the deformed quartz sand layers (Fig. 1b) were analyzed in order to study the effect of various parameters (stress, nature of the solution) on the kinetics of pressure solution (Gratier and Guiguet, 1986). Experimental pressure solution strain rates appeared to be limited by diffusion rates along stressed grain boundaries. These kinetic aspects are not discussed any further here. This paper focuses on scanning electron microscope (SEM) studies of the stressed grain contact that reveal micron-scale microstylolites along stressed grain-to-grain contacts. The microstylolite samples were obtained from two types of experiments, differing in the nature of the solution and their duration, namely, pure water for 51 days and aqueous NaOH 0.1 mole/l solution for 43 days. The change in shape of the grains by solution deposition is higher with NaOH 0.1 mole/l than with pure water (Gratier and Guiguet, 1986). However, as we will see below, the microstructures of dissolution are quite similar.

A general view of the quartz sand layers after deformation is shown in Fig. 2a. SEM photographs were taken directly on the samples. At this millimeter scale, small holes are visible in the initially polished quartzite support of the sand layer. When observed in thin sections (Fig. 1b), these holes were clearly related to localized dissolution along grain boundaries in the quartzite by sand grain indenters (Gratier and Guiguet, 1986). In Fig. 2b, a microstylolite surface appears well developed on the top of the grain, with peaks that are parallel to the direction of maximum compressive stress (σ_1). A slickolite (dissolution surface oblique to the displacement direction) has

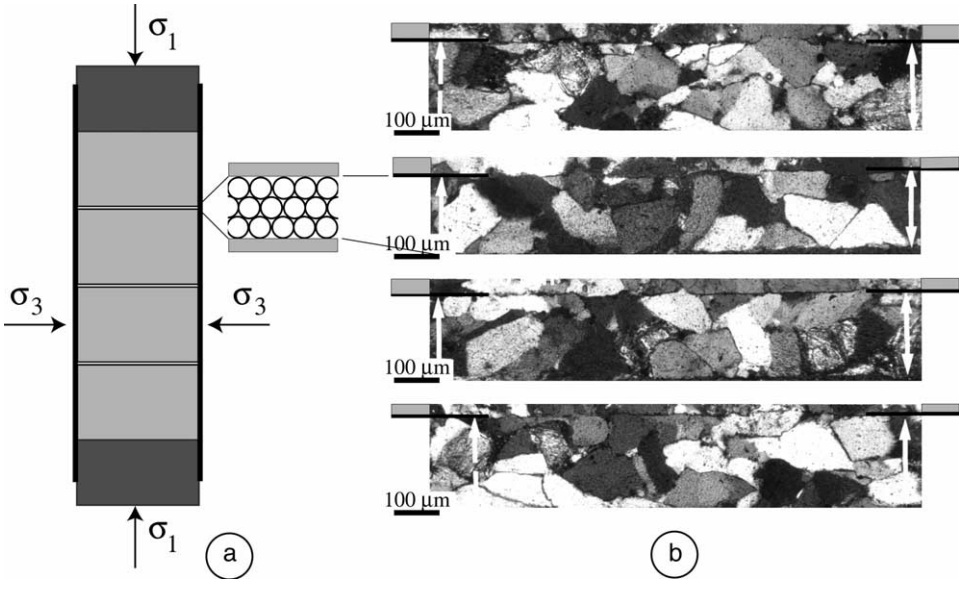

Fig. 1. (a) Schematic view of the experimental device: pressure vessel with permanent differential stress. σ_1 is the axial stress and σ_3 is the confining pressure that is also equal to the fluid pressure P. The sample assembly that was used in each experiment is a stack of four cylindrical blocks of quartzite between which were pressed three thin sand beds of small quartz grains (100–120 µm). (b) Thin sections that were made after the experiment: the white arrows indicate the boundary between the aggregate and the rigid plate (that was initially a flat polished surface) and also the direction of maximum compressive stress. Grain indentation attests to pressure solution processes. Heterogeneous dissolution of the rigid plate of quartzite (for example localized along grain boundaries in the quartzite) induces the development of a stylolitic structure of the quartzite/aggregate interface (interface underlined by thick black lines). The nature of the fluid was in this case a SiO_2 saturated Na OH 1 mole/l solution.

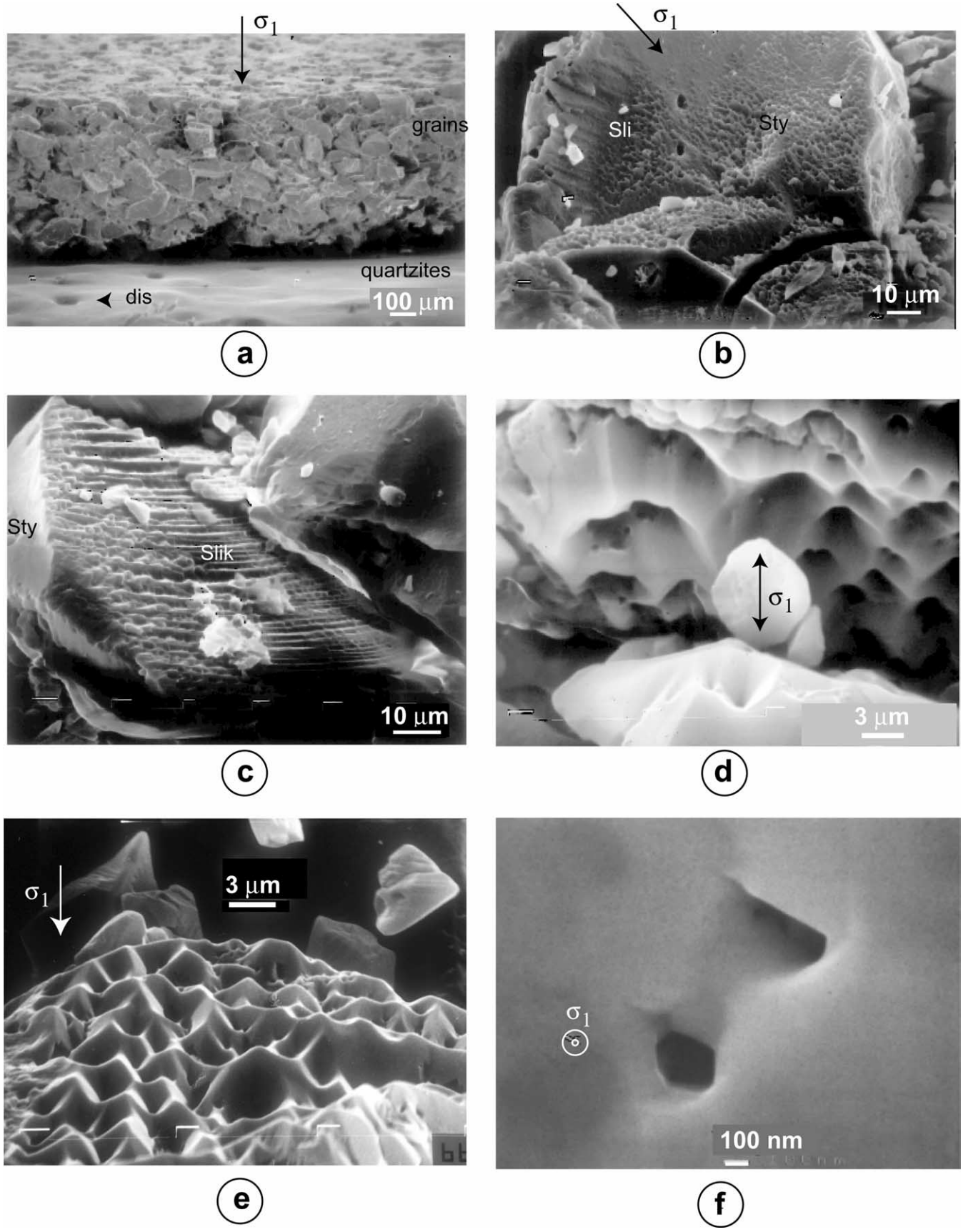

Fig. 2. Experimental microstylolites developed by a stress-driven dissolution process in the presence of various solutions: NaOH 0.1 M ((a), (b), (d) and (e)),

developed on the same grain in lateral continuity with the microstylolite surface, with its associated spikes also parallel to σ_1. Such patterns are observed only at grain contacts, the stress-free surfaces being flat and smooth. A more complex change in grain aggregate appears in Fig. 2c where a stylolitic surface abruptly changes into a slickenside structure. This change must have occurred as a result of the slight rotation of one of the grains after the development of the microstylolite. Most often, the surfaces of the grains, which are more or less parallel to σ_1 (grain boundaries or vertical fractures), show no evidence of microstylolites (Fig. 2b and c). Such near vertical surfaces, often open during sand compaction, create pore spaces that are filled with small euhedral quartz crystals (Gratier and Guiguet, 1986). However, in some very rare cases, microstylolites with horizontal peaks do develop on the vertical side of some grains, indicating local compressive stress oblique to the maximum stress. Like the microstylolite-to-slickenside transition already mentioned, such heterogeneous behavior may be related to a complex rearrangement of initially irregular grains during the progressive deformation. Throughout the samples, it can be seen that microstylolites develop both on top of and underneath each pair of stressed grains (Fig. 2d and e), in apparent symmetry, and without any visible mismatch along the seam. However, enlarging the view of the stylolitic surfaces reveals numerous dissolution pits that cross-cut the whole stylolitic dissolution surface (Fig. 2d; see Fig. 5e for a schematic view). These pits may be found all along the stylolitic surfaces. They are systematically located at the bottom of each conical-shaped indented stylolitic structure, which consequently looks like a funnel-shaped structure. Due to the fit of two opposite surfaces, the pits of the lower grain stylolitic surface are located just in front of the stylolitic peaks of the upper grain and vice versa. Detailed photographs of the pits (Fig. 2f) reveal their negative euhedral crystal shape, which resembles equilibrated fluid inclusions in quartz, possibly located at crystal dislocation outcrops.

Stereoscopic analysis of pairs of SEM photographs, processed in the same way and with the same resolution as topographic surfaces, yielded topographic data sets for two of these stylolitic surfaces. One of these surfaces is represented in Fig. 3b and c, in map and perspective view, respectively. Fourier analysis indicates that the surfaces are self-affine with a linear slope in a log–log diagram (Fig. 3d) (Meakin, 1998). The slope $\alpha = -3.5$ corresponds to a roughness exponent $H \approx 1.2$ ($\alpha = -1–2H$). Such high values for the roughness exponent have already been measured on natural stylolites at small scale (Renard et al., 2004; Schmittbuhl et al., 2004). Mean slopes of the peaks and depressed areas are equal on the two surfaces (around 36°) and there is no slope steeper than 65° (Fig. 3e).

3. Discussion of the experiments

At the grain scale (Fig. 2b), the parallelism between slickolite spikes and microstylolite peaks implies that the relative displacement vectors of the dissolution surface between two stressed grains are vertical, and parallel to σ_1. However, at a micron scale (Fig. 2d and e) the mean slope of the stylolitic surface is oblique to this displacement. This means that stress driven dissolution occurred, at least partially, on surfaces that were oblique to the main uniaxial loading stress. This observation is not specific to our experimental microstylolites. Observations of natural stylolites show a wide range of geometries (Park and Schot, 1968). Columnar stylolites have the simplest geometry, with column sides parallel to the displacement and column bases perpendicular to σ_1 (Fig. 4a). However, natural conical-shaped stylolites are also common (Fig. 4b). Note the close similarity between the natural stylolites and the experimental ones (respectively, Figs. 3c and 4b), despite a difference of four orders of magnitude in size between them. It has been suggested that columnar stylolites result from a coaxial stress history (as diagenetic stylolites), whereas conical-shaped stylolites are a product of non-coaxial stress history (Arthaud and Mattauer, 1969). Our experiments show that conical microstylolites can form through coaxial stress, therefore a non-coaxial history is not required for their formation. Observations at the highest magnification (Fig. 2f) also give information on the geometry of the grain-to-grain fluid interface: no evidence of channel and island structure, as described by Raj and Chyung (1981), Spiers and Schutjens (1990), and Cox and Paterson (1991), may be found at this scale. The trapped-fluid interface may best be termed as ‘pitted and waffled water-film’.

The striking feature of such experimental microstylolites is the systematic link between stylolitic peaks and dissolution pits. Pits may be seen all over the surface; however, they are systematically located in front of each peak (see Fig. 3a), with a polyhedral shape related to the crystalline structure (Fig. 2f). Such etch pits are commonly observed on mineral surfaces that have undergone aqueous dissolution. Such features have been shown to develop at the intersection of dislocations with the mineral surface (Frank, 1951; Mendelson, 1961; Brantley et al., 1986; Blum et al., 1990). The enhanced dissolution rate is presumably linked

pure water ((c) and (f)); see other parameters in the text. (a) General view of the quartz sand layer after deformation. (b) Microstylolite (sty) and slickolite (sli) on a single grain with peaks and spikes parallel to σ_1. (c) Microstylolitic surface that abruptly changes into slickenside structure after local grain rotation and friction. The near vertical surfaces of the grains were free of compressive stress and attest to their initial undeformed state. (d) Microstylolite on both bottom and top of stressed grains, respectively, that may be interpreted as a matching view of the same microstylolitic contact. (e) Typical microstylolitic surface found in the stressed aggregate. (f) Detail of dissolution pits developing in front of each microstylolite peak. The orientation of σ_1 relative to the surface is given on each picture.

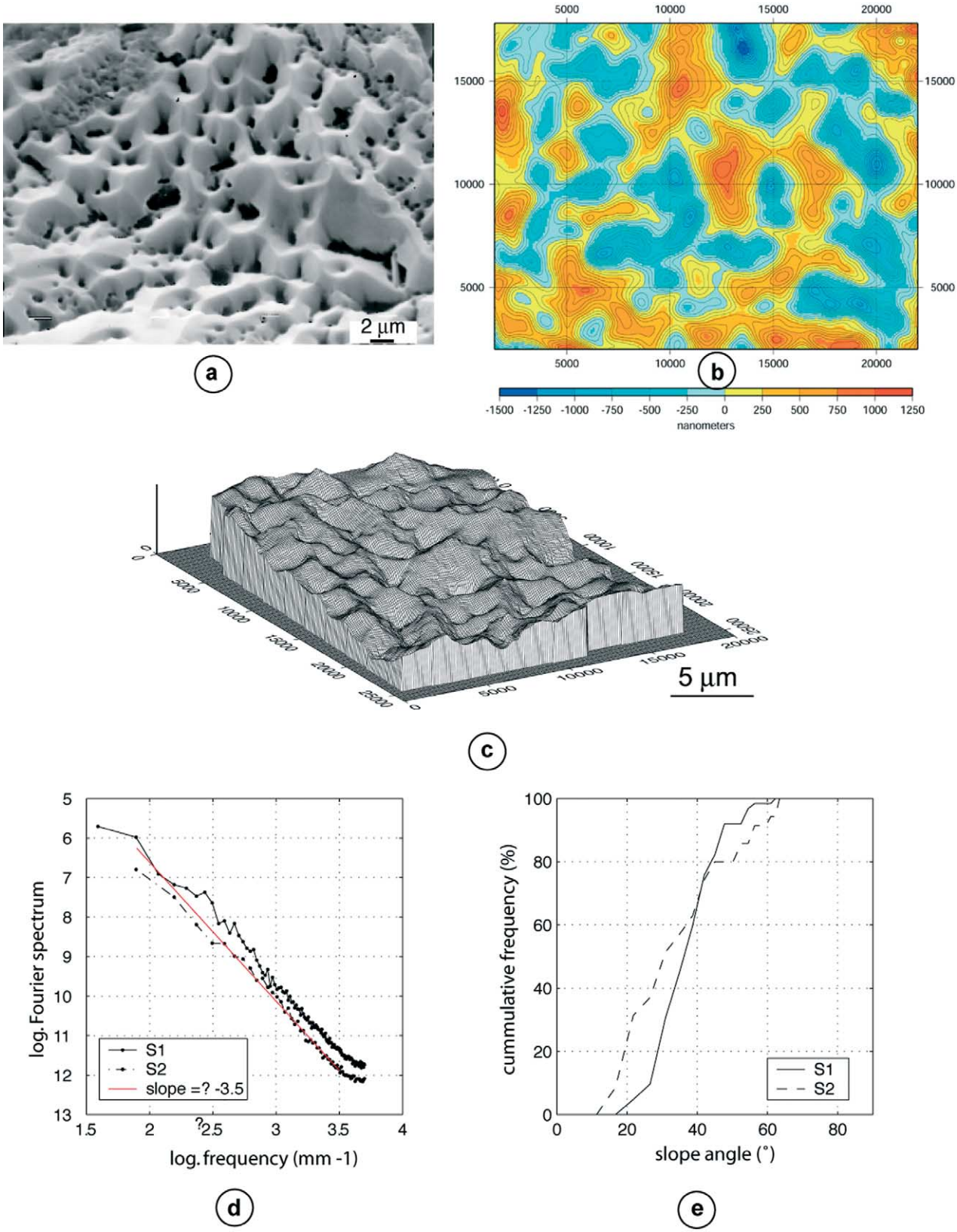

Fig. 3. Geometrical analysis of microstylolites. (a) Stereoscopic SEM photograph, view parallel to the experimental microstylolite peaks. (b) Structure contour map from stereoscopic restitution. (c) 3D perspective view of experimental microstylolite from stereoscopic restitution. (d) Spatial wavelength analysis of the microstylolite surface by Fourier transform. The surfaces are self-affine with a linear slope in this log–log diagram. The slope $\alpha = -3.5$ corresponds to a roughness exponent $H \approx 1.2$ ($\alpha = -1–2H$). (e) Cumulative distribution of the slopes on two different experimental microstylolite surfaces.

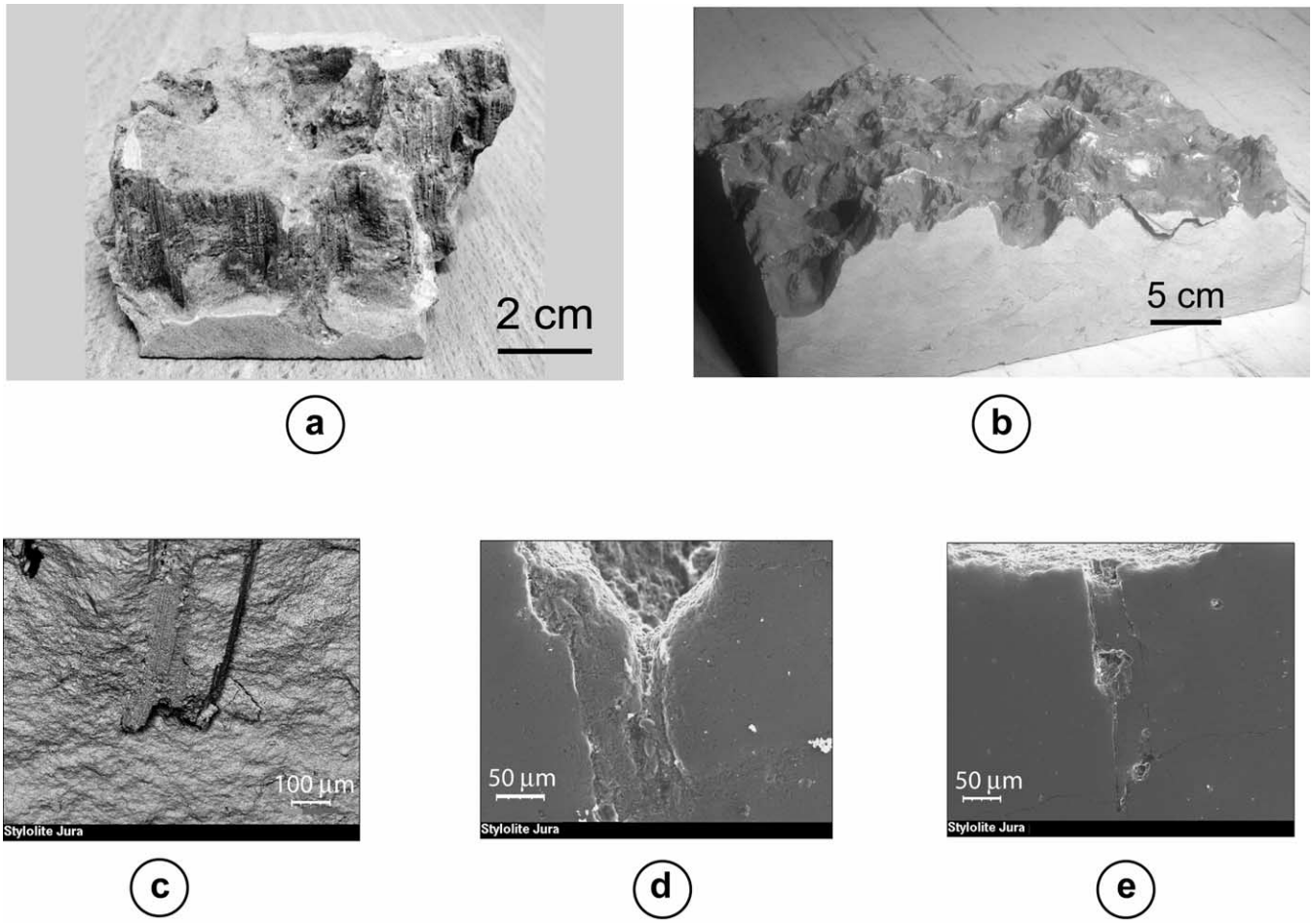

Fig. 4. Natural stylolites, with their shape varying from columnar stylolites (a) to conical stylolites (b), Cretaceous limestones, Chartreuse, French Alps. (c)–(e) Details of the shape of some columnar peaks, the column being bounded by vertical microfractures parallel to the σ_1 stress direction, Cretaceous limestone, Jura, French Alps.

to the high strain energy stored around the dislocations or to localized attack by the solvent on the geometric step on the crystal surface (Bosworth, 1981; Tada and Siever, 1986). Meike and Wenk (1988) also observed that voids and pits developed where dislocations emerged at the solution cleavage surface. Such voids and pits associated with dislocations concentration are interpreted as dissolution features that reflect the metastability of deformed parts of the crystal with respect to the perfect crystal in the presence of a fluid.

When assuming a plausible link between pits and dislocations, a rough analysis of etch pit density in Fig. 3a indicates a density of about 10^8 dislocations cm^{-2}. Such a value is compatible with dislocation densities in natural quartz that range from 10^5 to 10^{10} dislocations cm^{-2} (Blum et al., 1990). The lower dislocation density commonly appears during crystal growth, whereas higher density develops during plastic deformation of crystal. We are dealing here with crystals that had an initial low density of dislocations (euhedral crystals) but both crushing and indenting processes must have increased this density, leading to the observed value. Lines of high pit density are shown on Fig. 3a, and could reveal planar defects in the crystal probably related to the crystalline structure.

The systematic face-to-face coincidence of stylolitic peaks and dislocation may have several explanations. Dislocation pits may predate stylolitic development and their distribution could play a role in peak localization, or dislocation pits may develop after stylolitic amplification due to an indenter effect of the peaks. Although the second case cannot be excluded, some pits must predate the stylolitic development since pits are found, associated with small deflection, along the slope of the microstylolite peaks (Fig. 3a). We consider firstly that at least some dislocations predate the microstylolite development, secondly that dissolution pits were favored where the dislocations emerged at the grain surface, thirdly that such dissolution pits induce a slight deflection in the grain surface opposed to the one with the dissolution pit. This deflection initiates the microstylolite peak. In this case, heterogeneities in the crystal would control the development of the microstylolites. At another length scale this may be compared with the deflection of the quartzite/aggregate interface due to local dissolution of the quartzite plate, particularly at the sites of

grain boundaries and micro-fractures emergence (Fig. 1b). In summary, we will consider that when two stressed solids are pressed in contact, with their solution trapped in the interface, dissolution rates are heterogeneous and some rapidly developing pits can initiate slight deflections along the interface. Such deflections concentrate the stress and may amplify the development of the dissolution in front of each growing peak. At the same time, however, the effect of surface tension tends to smooth the surface. This is a stress-induced instability (for a review on such instability see, for example, Kassner et al. (2001)).

4. Principle of the modeling

A simple modeling approach is proposed, capable of generating stylolitic surfaces with a characteristic natural geometry ranging from conical-shaped to columnar-shaped stylolites (Fig. 4), as well as experimental geometry (Fig. 3). When considering the geometry of dissolution surfaces, there is a difference between conical and columnar stylolites: dissolution interfaces of columnar stylolites are disrupted by kinematic discontinuities parallel to the displacement (analogous to transfer faults; Fig. 5a), whereas conical stylolites show continuous (deflected) dissolution surfaces (Fig. 5b). However, transfer faults may also be associated with conical stylolites when they are larger than the peak size (such as the kinematic discontinuity shown in Fig. 2b, and schematically drawn in Fig. 5c).

The principle of our model is based on the experimental observation that dissolution pits are always located opposite to stylolite peaks. A fluid phase is considered to be trapped between two solids under stress (Fig. 5d). In addition, stress-induced dissolution rates are considered to be heterogeneously distributed along the two dissolution surfaces that are pressed together. For example, in experiments, dissolution rates near dislocation pits are higher than dissolution rates away from the dislocation pits because of the higher strain energy associated with each dislocation. At another scale, localized dissolution of the quartzite plates linked to some microstructures (grain boundary, micro-cracks) induces the deflection of the quartzite/aggregate interface (Fig. 1b). In natural deformation, the preferential dissolution zone may derive from an initially high porous area that determined the dissolution location, as in the self-organized model of stylolitic layering (Merino et al., 1983; Dewers and Ortoleva, 1990b). It may also derive from zones of high fracture density that are known to significantly enhance dissolution (Railsback and Andrews, 1995; Gratier et al., 1999). It may also be due to the effect of clay minerals that have been recognized to enhance pressure solution (Heald, 1955; Engelder and Marshak, 1985; Bjørkum, 1996; Renard et al., 1997).

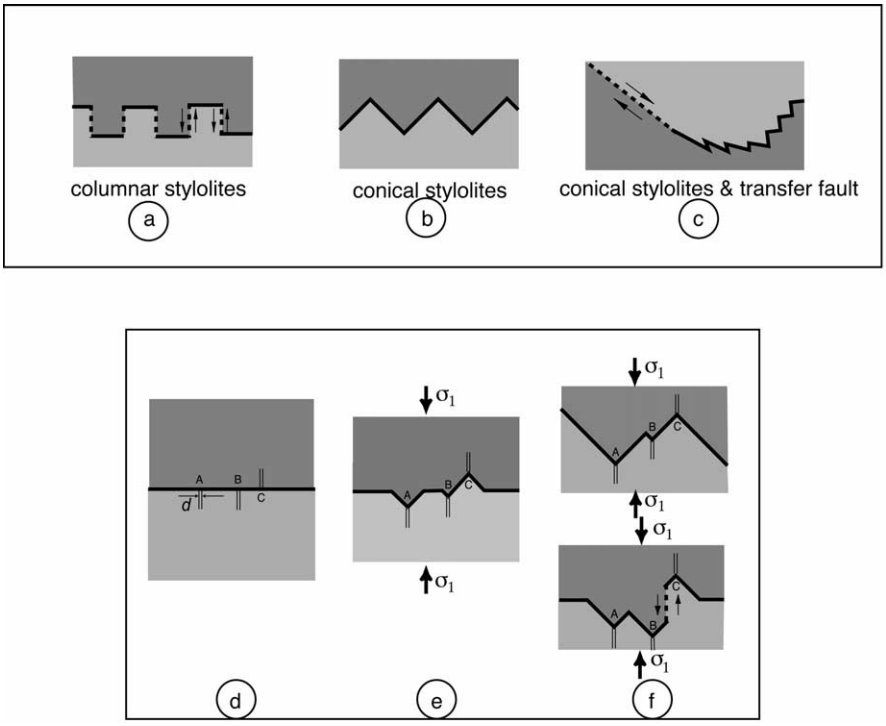

Fig. 5. Schematic view of stylolite development when two solids are pressed together with a solvent fluid phase trapped between dissolution surfaces, with the trapped fluid phase as thick lines and micro-tear faults as dashed lines. (a) Columnar stylolites: the dissolution surfaces are interrupted by micro-tear faults. (b) Conical stylolites: the dissolution surfaces are continuous. (c) Conical stylolites associated with transfer faults (schematic view of Fig. 2b). (d)–(f) Kinematic model of stylolite development as preferential dissolution sites, of diameter *d* and corresponding to the dissolution pits of Figs. 2f and 3a, which determine the stylolite peak location; two possibilities are presented with kinematic discontinuity (preexisting tension fracture) as transfer fault (bottom) or without such a discontinuity (top).

At all scales, the fastest dissolution sites along one of the surfaces generate a small deflection in the opposite surface due to the main compressive stress perpendicular to the solid–fluid–solid interfaces. This small deflection generates stress concentrations in the solid in a small zone opposite to the tip of the deflection (Jaeger and Cook, 1969). This increases the dissolution rate in the vicinity of the already preferential dissolution zone and leads to progressive growth of the stylolite peaks as a self-organized process. If both solid surfaces dissolve in symmetry, the shape of the stylolitic surface results from a complex interaction between the two solids and the dissolution-rate distribution.

A schematic view showing the change in microstylolites based on experimental observations is given in Fig. 5d–f. Points A–C are outcrops of dissolution pits along the two grain interfaces: dislocations A and B being in the lower grain and C in the upper grain. The dissolution trajectories are assumed to remain parallel to the general σ_1 direction. The various dissolution rates associated with different dislocation pits and the random distribution of these dislocation pits lead to a complex change in the microstylolite surface. For example (Fig. 5f-top), dislocation pit B (lower grain), with a relatively slow dissolution rate compared with that of dislocation C (upper grain) moves to the top of the microstylolite peak associated with dislocation C. Such geometry is well recognized in experiments (Figs. 2d and 3a). However, if sites B and C are both very active (fast dissolution, as in Fig. 5f-bottom) a kinematic discontinuity may develop, especially if the strength of the nearby solid is weak. This is seen in the experiment (Fig. 2b) where the slickolite surface ends up along transfer fault (model 5c). This arrangement is also common in natural stylolites when microfractures cut the rocks (see natural examples; Fig. 4c–e).

Consequently, modeling must take into account the strength of the solid interface around the preferential dissolution zones. A simplified approach is used, considering the mechanical equilibrium of a thin elastic membrane subjected to opposing vertical forces. The membrane is deformed by positive and negative incremental displacements of localized patches representing the fast-displacement dissolution areas in both the upper and lower grains, respectively. The displacement rates model the heterogeneous dissolution-rate distribution along the solid interface, promoting deflection. In parallel, the strength of the membrane inhibits the deflection and is opposed to its development. The principle of the model may be compared with the Asaro–Tiller–Grinfeld instability describing the geometry of a solid surface under stress and in contact with its melt. In this case, Asaro and Tiller (1972), Grinfeld (1986) and Kassner et al. (2001) showed that when accidental corrugations develop at the solid–fluid surface, two processes are competing to increase or anneal the deflection: elastic energy stored in the solid tends to develop surface deflection, whereas surface energy limits the development of a rough surface.

Our modeling algorithm is derived as follows:

1. Fast dissolution patches of fixed diameter '*d*' (Fig. 5c) are randomly distributed over the entire surface.
2. Half of these patches are associated with upward displacement (upward forces), the other half being associated with downward displacement (downward forces).
3. At each incremental step in the loading process, only randomly selected patches are displaced in order to simulate the heterogeneity of the dissolution-rate distribution. This is similar to the principle of 'game of life' models (Gardtner, 1970), in particular when used to model self-organized systems (Bak and Tang, 1989).
4. The elastic properties of the solid are kept constant throughout the whole process.

At each increment, the thin elastic membrane is loaded by vertical forces and subjected to buoyant restoring forces on its two faces by elastic springs. The vertical displacement field $u(x,y)$ of the membrane is then governed by the differential equation:

$$F = \tau(d^2u/dx^2 + d^2u/dy^2) + ku \quad (1)$$

where F is the vertical density of force (N/m^2); τ is the stiffness of the membrane (N/m) and is equivalent to a surface tension and ku is the restoring force. The parameter k which can be interpreted as the 'stiffness' of the springs (force per unit volume: N/m^3) represents the characteristics of the dissolution process (ratio F/u, if τ is negligible). The stiffness of the membrane τ stands for the stiffness of the rock along the dissolution interface. The spatial load distribution $F(x,y)$ represents the random geometry of the fast dissolution patches. Only two parameters allow the reproduction of the variety of stylolite geometries: the ratio k/τ and the spatial distribution of the patches $F(x,y)$.

This model differs from the kinematical models of stylolites that described stylolitic development by random dissolution on one side or the other of the dissolution surface (Guzetta, 1984), or that depend on the spatial distribution of porosity (Andrews and Railsback, 1997). In our model the competition between the process that activates the

Fig. 6. Simplified mechanical modeling of the stylolite process: modeled conical stylolites with eight successive loading increments. (a) Random geometry of fast dissolution patches at each step (the red ones are associated with upward displacement, the blue ones with downward displacement). (b) Perspective views of three steps (S1, S4, S8). (c) Fourier spectrum of these modeled stylolite surfaces: the FFT spectrum of the eight surfaces (S1–S8) at different stages of stylolite development indicates a self-similar geometry over more than one order of magnitude of wavenumbers. The roughness $H \approx 1.2$, corresponding to a slope of -3.5 is close to what has been observed on the experimental microstylolites (Fig. 3).

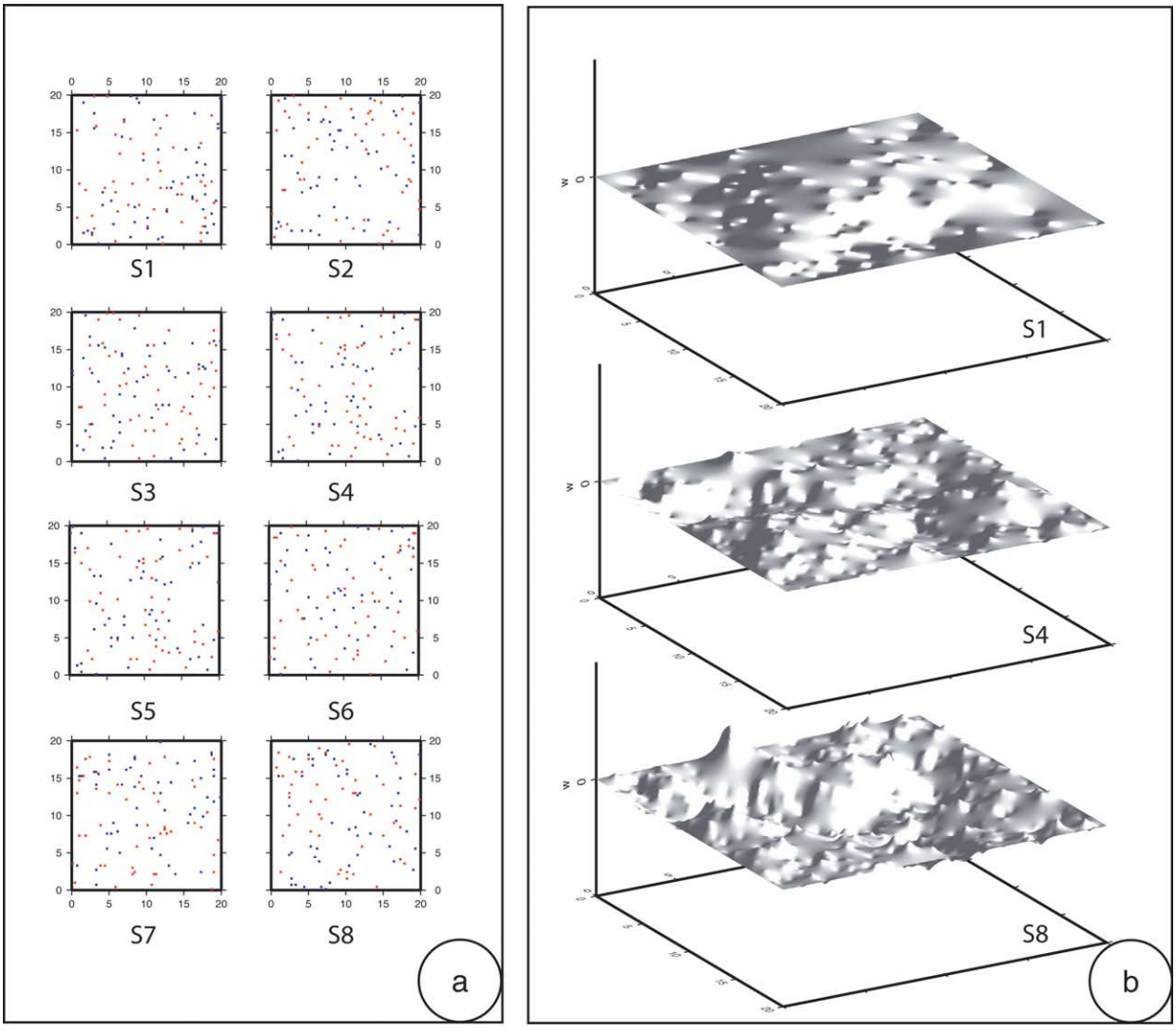
S1
S2
S3
S4
S5
S6
S7
S8
a
w
S1
S4
S8
b

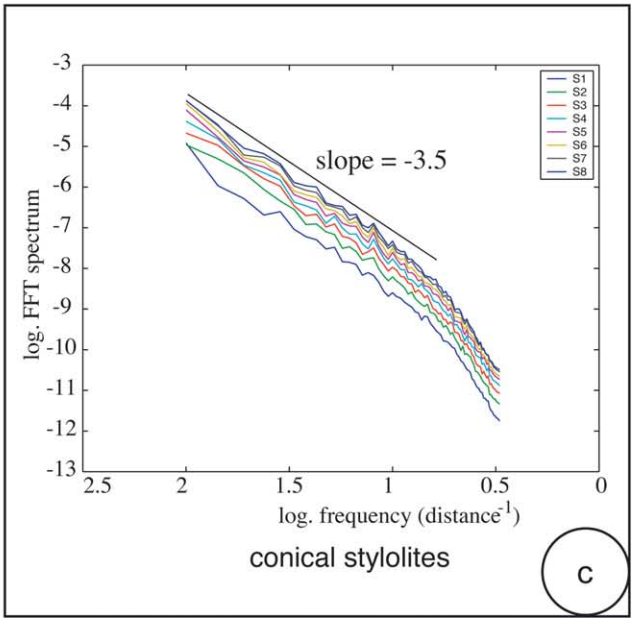
slope = -3.5
log. FFT spectrum
log. frequency (distance-1)
S1
S2
S3
S4
S5
S6
S7
S8
conical stylolites
c

development of the peaks (localized dissolution) and the process that limits their development (stiffness of the rock) mimics the Asaro–Tiller–Grinfeld instability based on a competition between stress-activated free-energy that destabilizes the surface (here by dissolution), and surface energy that tends to smooth it. Modeling the mechanical equilibrium of a thin elastic membrane is a first approach that allows us to evaluate the result of theses two competing effects at various scales.

5. Discussion of the models

Modeling results are presented in Fig. 6a and b. Two types of structures are obtained that represent two types of stylolite geometry. Conical stylolites developed in several increments, for example from 400 initial small patches (half with positive forces, half with negative ones) as shown in Fig. 6a. Perspective views show the progressive development of such stylolite surfaces (Fig. 6b). The specific characteristic of experimental microstylolites can be seen. The largest stylolite peaks and conical depressed areas develop in front of the most active dissolution pits (positive and negative, respectively). Secondary peaks and depressed areas of smaller size are seen all along the surface corresponding to less active dissolution sites. A complex organization emerges from such a simple modeling that will be analyzed more carefully in the future. With such a simplified mechanical model, the vertical displacement represents the ratio between force and stiffness. The Fourier analysis of the modeled 'stylolite' surfaces indicates that the roughness exponent is high ($H \approx 1.2$; see Fig. 6c), close to the value found for experimental microstylolites. This high value, greater than one, is also found by Renard et al. (2004) and Schmittbuhl et al. (2004), by spectral analysis of natural stylolites at small scale. Karcz and Scholz (2003) found lower values of this roughness exponent for natural stylolite: H ranging from 0.53 to 0.74. Renard et al. (2004) and Schmittbuhl et al. (2004) show that self-affine fractal roughness of natural stylolites presents a well characterized crossover length scale separating two self-affine regimes: $H \approx 1.1$ (at small length scale, mm–μm) and $H \approx 0.5$ (at larger length scale). These authors modeled the complex 2D stylolite morphology as the result of a competition between the long-range elastic redistribution of local stress fluctuation, which roughen the surface, and surface tension forces along the interface, that smooth it. The change in self-affine regime expressed the evolution of the balance between the elastic forces on the interface and the capillarity forces: the 'mechanical' regime, with $H \approx 0.5$, is dominant at large length scale (mm–dm) whereas the 'capillarity' regime, with $H \approx 1.1$, dominates at small length scale processes (μm–mm). This latter value is similar to the one obtained here for our 3D modeling of conical stylolites that integrates a strong 'tension surface' effect.

Our simplified modeling aims at reproducing the main characteristics of the shape of the stylolites with the minimum number of parameters, namely two main parameters: heterogeneous dissolution-rate distribution (spatial load distribution) and simplified mechanical properties of the solid (membrane stiffness). Modeling results (Figs. 6 and 7) show the effect of these two parameters on stylolite geometry. Columnar stylolites (Fig. 7) are obtained both when using a smaller number and a larger size of patches of fast dissolution and when using a much lower stiffness of the elastic membrane than for conical stylolites (Fig. 6). This clear difference provides information on dissolution-site heterogeneity (size and distribution) and mechanical behavior of the rocks during stylolite development. According to this model, columnar stylolites indicate much lower grain interface stiffness than conical stylolites. This low stiffness may be associated either with poorly lithified sediment at the beginning of the diagenetic process, or with tension fractures parallel to the maximum compressive stress that have no shear strength parallel to the potential transfer fault (Fig. 4c–e). The processes that impose the fast dissolution patches probably vary with the size of the stylolites. It may be dislocation-related dissolution pits at micron scale in experiments (Fig. 2). For natural stylolites, it may also be imposed by some high porosity or high fracture density zones at various scales (Den Brok, 1998; Gratier et al., 1999), or by the effect of any initial heterogeneity (e.g. fossils, nodules), or by the presence of clay minerals that enhance dissolution (Fig. 4). Greater complexity is expected if a solid developing conical stylolites is considered (numerous localized dissolution patches and high stiffness of the solid) when the solid includes preexisting fractures that may

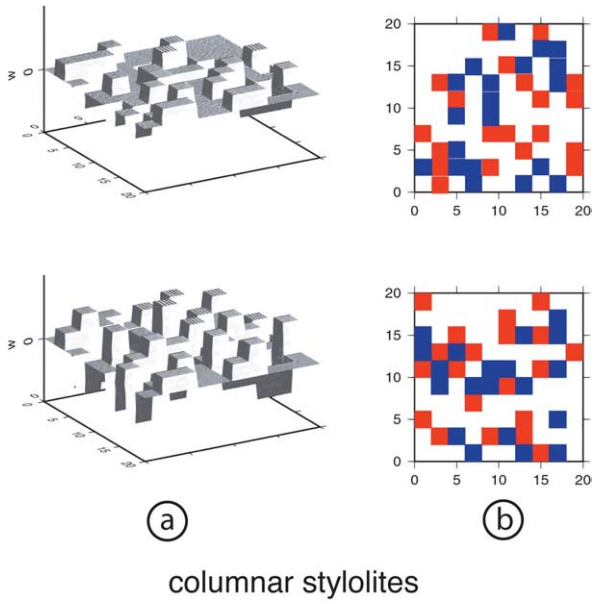

Fig. 7. Simplified mechanical modeling of the stylolite process: modeled columnar stylolites. (a) Perspective views. (b) Distribution of preferential dissolution sites (the red ones are associated with upward displacement, the blue ones with downward displacement).

develop into kinematic discontinuities (Figs. 2b, 4a and 5c and f), or when we take into account the progressive evolution of rock properties with mass transfer that are associated with deformation (Gratier, 1987).

6. Conclusion

Experimental microstylolites have been observed at stressed contacts between quartz grains loaded for a period of several months in the presence of an aqueous silica solution, at 350 °C under 50 MPa of differential stress. SEM images and the derived microstylolite topography reveal that the complex geometry of microstylolite surfaces is imposed by the interplay between the development of dissolution peaks in preferential locations (dissolution pits) and the mechanical properties of the solid–fluid–solid interfaces. Spectral analyses of some experimental microstylolites reveal a self-affine roughness (roughness exponent $H \approx 1.2$).

Simple mechanical modeling produces stylolitic surfaces with characteristic geometries that vary from conical to columnar shaped stylolites when both the effects of dissolution-rate heterogeneity and mechanical properties of the rock are included.

Experiment and discrete modeling enable the role of two main parameters in the development of stylolitic geometry to be distinguished:

1. The initial distribution of heterogeneous dissolution-rate areas along the interface localizes the first stylolite peaks and controls the progressive deflection of the dissolution surface.
2. The mechanical properties of the stressed solid impose the slope of the dissolution surfaces around the preferential dissolution zones.

The model expresses a crucial competition that may govern the development of stylolites:

1. A stress related process modeled in terms of the stiffness of springs activates the heterogeneous displacement rates of the solid interface that promotes deflection.
2. The strength of the solid interface, modeled in terms of the stiffness of a membrane, and equivalent to a surface tension, limits the deflection and is opposed to its development.

Interaction between these two main parameters in the model leads to various geometrical shapes of stylolite surfaces. Heterogeneous dissolution promotes wavelength and amplitude variations of the stylolites. Spectral analyses of such modeled stylolites reveal a self-affine roughness, with a roughness exponent ($H \approx 1.2$) that is comparable with experimental microstylolites and small length scale natural stylolites.

In this model, conical stylolites develop with high solid stiffness and with relatively localized patches of fast dissolution (as dissolution pits in experiments or localized spots in natural stylolites). Columnar stylolites develop with low solid stiffness and with relatively large patches of fast dissolution patches (for example in relation to heterogeneous compaction or to rock fracturing process). A mixed model of conical stylolites associated with fault transfer may also develop with high-stiffness solids cut by tensile fractures that develop into kinematic discontinuities. The modeling could then reproduce the main characteristics of both experimental microstylolites and natural stylolitic structures.

Acknowledgements

We thank R. Guiguet and L. Jenatton for their technical help. B. Railsback and Z.K. Karcz for their fruitful reviews and Tom Blenkinsop for his final help.

References

Andrews, L.M., Railsback, L.B., 1997. Controls on stylolite development: morphologic, lithologic, and temporal evidence from bedding-parallel and transverse stylolites from the U.S. Appalachians. Journal of Geology 105, 59–73.

Arthaud, F., Mattauer, M., 1969. Exemples de stylolites d'origine tectonique dans le Languedoc, leur relation avec la tectonique cassante. Bulletin de la Société Géologique de France 11, 738–744.

Asaro, R., Tiller, W., 1972. Interface morphology development during stress corrosion cracking: part 1, via surface diffusion. Metallurgical and Materials Transactions 3, 1789–1796.

Bak, P., Tang, C., 1989. Earthquakes as a self-organized critical phenomenon. Journal of Geophysical Research 94, 16635–16637.

Bathurst, R.G.C., 1971. Carbonate Sediments and their Diagenesis. Elsevier, Amsterdam.

Bjørkum, P.A., 1996. How important is pressure in causing dissolution of quartz in sandstones? Journal of Sedimentary Research 66, 147–154.

Blum, A., Yund, R., Lasaga, A., 1990. The effect of dislocation density on the dissolution rate of quartz. Geochimica Cosmochimica Acta 54, 283–297.

Bosworth, W., 1981. Strain-induced preferential dissolution of halite. Tectonophysics 78, 509–525.

Brantley, S.L., Crane, S., Crerar, D., Hellman, R., Stallard, R., 1986. Dissolution at dislocation etch pits in quartz. Geochimica Cosmochimica Acta 50, 2349–2361.

Carrio-Schaffhauser, E., Raynaud, S., Latière, H.J., Mazerolles, F., 1990. Propagation and localization of stylolites in limestones, in: Knipe, R.J., Rutter, E.H. (Eds.), Deformation Mechanisms, Rheology and Tectonics Geological Society Special Publication, 54, pp. 193–199.

Cox, S.F., Paterson, M.S., 1991. Experimental dissolution–precipitation creep in quartz aggregates at high temperatures. Geophysical Research Letters 78, 1401–1404.

Deelman, J.C., 1976. Lithification analysis: experimental observations. Geologische Rundschau 65, 1055–1078.

Den Brok, S.W.J., 1998. Effect of microcracking on pressure solution strain rate: the Gratz grain-boundary model. Geology 26, 915–918.

Dewers, T., Ortoleva, P., 1990a. A coupled reaction/transport/mechanical

model for intergranular pressure solution stylolites, and differential compaction and cementation in clean sandstones. Geochimica Cosmochimica Acta 54, 1609–1625.

Dewers, T., Ortoleva, P., 1990b. Interaction of reaction, mass transport, and rock deformation during diagenesis, mathematical modeling of intergranular pressure solution, stylolites and differential compaction cementation, in: Ortoleva, P. (Ed.), Prediction of Reservoir Quality through Chemical Modeling AAPG Memoir, 49, pp. 147–160.

Dunnington, H.V., 1954. Stylolites development post-date rock induration. Journal of Sedimentary Petrology 24, 27–49.

Engelder, T., Marshak, S., 1985. Disjunctive cleavage formed at shallow depths in sedimentary rocks. Journal of Structural Geology 7, 327–343.

Frank, F.C., 1951. Capillary equilibria of dislocated crystals. Acta Crystallographia 4, 497–501.

Gardtner, M., 1970. Mathematical game. The fantastic combinations of John Conroy's new solitaire game "life". Scientific American 223, 120–120.

Gratier, J.P., 1987. Pressure solution–deposition creep and associated tectonic differentiation in sedimentary rocks, in: Jones, M.E., Preston, R.M.F. (Eds.), Deformation of Sediments and Sedimentary Rocks Geological Society of London Special Publication, 29, pp. 25–38.

Gratier, J.P., Guiguet, R., 1986. Experimental pressure solution–deposition on quartz grains: the crucial effect of the nature of the fluid. Journal of Structural Geology 8, 845–856.

Gratier, J.P., Renard, F., Labaume, P., 1999. How pressure-solution and fractures interact in the upper crust to make it behave in both a brittle and viscous manner. Journal of Structural Geology 21, 1189–1197.

Grinfeld, M.A., 1986. Instability of the separation boundary between a non-hydrostatically stressed solid and a melt. Sov. Phys. Dokl. 31, 831.

Guzetta, G., 1984. Kinematics of stylolite formation and physics of the pressure-solution process. Tectonophysics 101, 383–394.

Heald, M.T., 1955. Stylolites in sandstones. The Journal of Geology 63, 101–114.

Jaeger, J.C., Cook, N.G.W., 1969. Fundamentals of Rock Mechanics. Methuen & Co.

Karcz, Z., Scholz, C.H., 2003. The fractal geometry of some stylolites from the Calcare Massiccio Formation, Italy. Journal of Structural Geology 25, 1301–1316.

Kassner, K., Misbah, C., Muller, J., Kappey, J., Kohlert, ?, 2001. Phase-field modeling of stress-induced instabilities. Physical Review E 63, 0361171/27.

Meakin, P., 1998. Scaling and Growth far from Equilibrium. Cambridge University Press.

Meike, A., Wenk, H.-R., 1988. A TEM study of microstructures associated with solution cleavage in limestone. Tectonophysics 154, 137–148.

Mendelson, S., 1961. Dislocation etch pit formation in sodium chlorite. Journal of Applied Physics 32, 1579–1583.

Merino, E., Ortoleva, P., Strickholm, P., 1983. Generation of evenly spaced pressure solution seems during late diagenesis: a kinetics theory. Contributions to Mineralogy and Petrology 82, 360–370.

Milliken, K.L., 1994. The widespread occurrence of healed microfractures in siliclastic rocks: evidence from scanned cathodoluminescence imaging. In: Nelson, P.P., Laubach, S.E. (Eds.), Rock Mechanics. Balkema, Rotterdam.

Park, W.C., Schot, E.H., 1968. Stylolites, their nature and origin. Journal of Sedimentary Petrology 38, 175/1.

Raj, R., Chyung, C.K., 1981. Solution–precipitation creep in glass ceramics. Acta Metallurgica 29, 159–166.

Railsback, L.B., 1998. Evaluation of spacing of stylolites and its implication for self-organizations of pressure dissolution. Journal of Sedimentary Petrology 68, 2–7.

Railsback, L.B., Andrews, L.M., 1995. Tectonic stylolites in the undeformed Cumberland Plateau of southern Tennessee. Journal of Structural Geology 17, 911–915.

Renard, F., Ortoleva, P., Gratier, J.P., 1997. Pressure solution in sandstones: influence of clays and dependence on temperature and stress. Tectonophysics 280, 257–266.

Renard, T., Schmittbuhl, J., Gratier, J.P., Meakin, P., Merino, E., 2004. Three-dimensionnal roughness of stylolites in limestones. Journal of Geophysical Research 109, B03209.

Rutter, E.H., 1976. The kinetics of rock deformation by pressure solution. Philosophical Transactions of the Royal Society of London 283, 203–219.

Schmittbuhl, J., Renard, F., Gratier, J.P., 2004. The roughness of stylolites: implication of 3D high resolution topography measurements. Physical Review Letters, in revision.

Spiers, C.J., Schutjens, P.M.T.M., 1990. Densification behaviour of wet granular salt: theory versus experiment. In: Seventh Symposium on Salt, Elsevier Sciences, Amsterdam, vol. 1, pp. 83–92.

Stockdale, P.B., 1922. Stylolites: Their Nature and Origin. Indiana University Studies.

Tada, R., Siever, R., 1986. Experimental knife-edge pressure solution of halite. Geochimica Cosmochimica Acta 50, 29–36.